Research Square

Preprints are preliminary reports that have not undergone peer review.
They should not be considered conclusive, used to inform clinical practice,
or referenced by the media as validated information.

The cell adhesion receptor TMIGD1 recruits Scribble to the basolateral membrane via direct interaction

Klaus Ebnet (ebnetk@uni-muenster.de)
University of Muenster https://orcid.org/0000-0002-0417-7888
Eva-Maria Thüring
University of Muenster https://orcid.org/0000-0002-7984-4171
Christian Hartmann
University of Muenster
Janesha Maddumage
Airah Javorsky
Birgitta Michels
Volker Gerke
University of Münster https://orcid.org/0000-0001-7208-8206
Lawrence Banks
Patrick Humbert
La Trobe University https://orcid.org/0000-0002-1366-6691
Marc Kvansakul
La Trobe University https://orcid.org/0000-0003-2639-2498

Article

Keywords: TMIGD1, cell adhesion molecule, cell-cell adhesion, polarity, Scribble, tumor suppressor

Posted Date: March 16th, 2023

DOI: https://doi.org/10.21203/rs.3.rs-2639220/v1

License: This work is licensed under a Creative Commons Attribution 4.0 International License.
Read Full License

Abstract

Scribble (Scrib) is a multidomain polarity protein and member of the leucine-rich repeat (LRR) and PDZ domain (LAP) protein family. A loss of Scrib expression is associated with disturbed apical-basal polarity and tumor formation. The tumor suppressive activity of Scrib depends on its membrane localization. However, despite the identification of numerous Scrib-interacting proteins, the mechanisms regulating its membrane recruitment are unclear. Here, we identify the cell adhesion receptor TMIGD1 as a membrane anchor of Scrib. TMIGD1 directly interacts with Scrib through a PDZ domain-mediated interaction. We characterize the association of the TMIGD1 C-terminus with each Scrib PDZ domain and describe the crystal structure of the TMIGD1 peptide – Scrib PDZ1 complex. We also find that TMIGD1 recruits Scrib to the lateral membrane domain when the LRR region is absent. Our findings describe a mechanism of Scrib membrane localization and contribute to the understanding of the tumor suppressive activity of Scrib.

Introduction

The apico-basal membrane polarity of epithelial cells is determined by three distinct membrane domains: the apical domain facing the lumen of an organ or the outside of a tissue, the lateral domain contacting adjacent cells, and the basal domain adhering to the extracellular matrix (ECM) [1]. The three domains differ in the composition of proteins and lipids to achieve their specific functions, including the formation of a brush border in the apical membrane domain, the regulation of cell-cell cohesion at the lateral membrane domain, and the regulation of cell-matrix adhesion at the basal membrane domain. The development and maintenance of apical-basal polarity is critical, as a loss of cell-cell or cell-matrix adhesion contributes to uncontrolled growth and, eventually, to metastasis, unless counter-regulated by cell death mechanisms such as anoikis [2]. Importantly, the establishment of membrane polarity is a dynamic process. For example, during development or wound healing some epithelial cells lose apical-basal membrane polarity, adopt mesenchymal characteristics, and migrate to distant sites, a process called epithelial-to-mesenchymal transition (EMT) [3]. Conversely, mesenchymal cells can re-polarize at distant sites to form new epithelial tissues [4, 5]. Given that transitions between epithelial and mesenchymal states are critical for the induction of normal and also of neoplastic stem cells from somatic cells [5, 6], the development of apical-basal polarity must be tightly controlled to prevent neoplastic transformation.

Epithelial apical-basal polarity is regulated by a conserved set of polarity proteins which are organized around three major cell polarity protein complexes. These include the Crumbs – Pals1 – PATJ complex (Crumbs complex), the PAR-3 – aPKC – PAR-6 complex (PAR – aPKC complex), and the Scribble – Dlg – Lgl complex (Scrib complex) [1, 7]. During the development of apical-basal polarity, the composition of these three polarity complexes is dynamically regulated and involves mutual interactions and changes in their composition [1, 8]. In fully polarized epithelial cells, the Crumbs complex, together with a PAR-6 – aPKC complex, localizes to the apical membrane; PAR-3 is localized at the tight junction, which

demarcates the border between apical and lateral membrane domains; and the Scrib complex is localized at the lateral membrane domain [1, 9]. The mutually exclusive localization of the polarity proteins is regulated by antagonistic interactions. For example, phosphorylation of PAR-3 by the PAR-6 – aPKC complex prevents the formation of a PAR-3 – aPKC – PAR-6 complex at the apical membrane [10, 11], and the polarity kinase PAR-1 inactivates PAR-3 to prevent the formation of a stable PAR-3 – aPKC – PAR-6 complex at the lateral membrane [12].

Given the critical role of epithelial apical-basal polarity in the maintenance of tissue homeostasis it is not surprising that polarity signaling is often dysregulated in cancer [13, 14]. Among the polarity proteins involved in tumorigenesis, Scrib stands out, as its downregulation has been reported in a large variety of tumors [15, 16]. Its pleiotropic functions in suppressing tumor formation can partly be explained by its ability to interact with a plethora of binding partners [15, 17], through which Scrib impacts on several signaling pathways involved in cell proliferation and cell migration. These pathways include Hippo signaling, RAS – MEK – ERK signaling, JNK – p38 signaling, and PI3K – Akt signaling [15]. Importantly, mislocalization transforms Scrib from a membrane-associated tumor suppressor to a cytosolic driver of tumor formation [18, 19], indicating that membrane localization is key to its tumor-suppressing activity. Despite this critical role of membrane localization, the mechanisms of membrane recruitment are still unclear [17]. Scribble comprises of 16 Leucine-Rich Repeats (LRR), two LRR and PSD95/Dlg/ZO-1 (PDZ)-specific domains (LAPSD), and four PDZ domains [16]. While a few interactions are mediated by the LRR region and the C-terminal region, the vast majority of interactions of Scribble are mediated via the PDZ domains, typically by binding a PDZ domain-binding motif (PBM) found at the extreme C-terminus of an interacting protein in the conserved ligand binding groove in the PDZ domain [15, 17]. A cell adhesion receptor at the lateral membrane domain of epithelial cells that recruits Scrib has not been identified.

Transmembrane and immunoglobulin domain-containing protein 1 (TMIGD1) is a cell adhesion receptor of the immunoglobulin (Ig) family whose expression is successively downregulated during the progression of normal colonic tissue to colorectal cancer tissue [20, 21]. TMIGD1 is predominantly expressed by proximal tubule kidney epithelial cells [21, 22, 23], and by intestinal epithelial cells [24, 25, 26]. In kidney epithelial cells grown at low density, TMIGD1 localizes to mitochondria [23]. In intestinal epithelial cells TMIGD1 localizes to the brush border and regulates microvilli organization [24, 26]. In almost all other tissues TMIGD1 mRNA or protein expression is hardly detectable (https://www.proteinatlas.org/ENSG00000182271-TMIGD1/tissue) [22]. Also, in many cultured cell lines derived from different tissues, TMIGD1 expression is very low [20].

In this study, we identify TMIGD1 as a binding partner for Scrib. We find that TMIGD1 interacts directly with Scrib in a manner that involves PDZ domains of Scrib and the PBM of TMIGD1. We describe the crystal structure of the Scrib PDZ1 domain complexed with a C-terminal TMIGD1 PBM peptide. We show that TMIGD1 can recruit Scrib to the lateral membrane domain and that expression of a dominant-negative TMIGD1 mutant disturbs three-dimensional cyst morphogenesis. Our findings identify an

adhesion receptor at the lateral membrane of polarized epithelial cells which directly binds Scrib, and they provide a structural basis for the mechanisms regulating Scrib membrane recruitment in epithelial cells.

Results

Scribble interacts with the cell adhesion receptor TMIGD1

In a search for cytoplasmic binding partners of TMIGD1, we performed a yeast-two hybrid experiment using the cytoplasmic domain of TMIGD1 as bait and a murine embryonic cDNA library [27]. In two independent screens, several overlapping clones were identified which covered a total region encoding AA633 to AA836 of murine Scrib (Fig. 1A). These findings suggested a direct interaction of TMIGD1 with the first PDZ domain of Scrib. GST-pulldown experiments with the cytoplasmic tail of TMIGD1 fused to GST and a recombinant Scrib construct containing the PDZ domain region of Scrib (Scrib/PDZ) confirmed a strong interaction of TMIGD1 with the Scrib PDZ domains that was lost after deletion of the C-terminal PBM of TMIGD1 (-SETAL) (Fig. 1B).

In many cultured polarized epithelial cells including Caco2 cells, T84 cells and MDCK cells, TMIGD1 is expressed by only a small subset of cells or not at all [26]. We therefore expressed TMIGD1 exogenously in HEK293 cells and analysed its interaction with endogenous Scrib by co-immunoprecipitation (CoIP). Scrib was present in TMIGD1 full length (TMIGD1/f.l.) precipitates but not in TMIGD1/Δ5 precipitates, indicating that TMIGD1 interacts with Scrib in a PBM-dependent manner in cells (Fig. 1C). Since this interaction was weak, despite the strong interaction observed with recombinant proteins (Fig. 1B), we ectopically expressed both TMIGD1 and Scrib in HEK293 cells and performed CoIP experiments in the presence of TAK-243, an inhibitor of Ubiquitin-activating enzyme E1 (UBE1), the mammalian E1 enzyme that charges the vast majority of E2 ubiquitin-conjugation enzymes with ubiquitin [28]. TAK-243 treatment increased the expression levels of both TMIGD1 and Scrib and enhanced the interaction of Scrib with TMIGD1 (Fig. 1D). These findings indicated that both TMIGD1 and Scrib are subject to proteasomal degradation in HEK293 cells.

To further characterize the interaction between TMIGD1 and Scrib we performed CoIP experiments from HEK293 cells expressing various Scrib deletion constructs (Fig. 2A - D). A Scrib full length (Scrib/f.l.) construct interacted with TMIGD1/f.l. but not with TMIGD1/Δ5 (Fig. 2B). Similarly, a Scrib construct consisting of the four PDZ domains (Scrib/PDZ) as well as a Scrib/PDZ construct with a C-terminal CAAX motif for membrane targeting (Scrib/PDZ-CAAX) interacted with TMIGD1 in a PBM-dependent manner (Fig. 2C). A Scrib construct consisting of the LRR region alone did not interact with TMIGD1 (Fig. 2D). These findings indicated that TMIGD1 and Scrib interact in cells in a manner that involves the PBM of TMIGD1 and the PDZ domain region of Scrib.

To address the specificity of this interaction among the LAP family members [16] we analyzed the interaction of TMIGD1 with Erbin and Lano/LRRC1 (Fig. 2E). We did not observe an association between

TMIGD1 and Erbin or Lano/LRRC1 by CoIP suggesting that TMIGD1 interacts specifically with Scrib among the LAP family members that are expressed in epithelial cells.

Scribble PDZ1 interacts with TMIGD1 through a canonical PDZ interaction

The yeast-two hybrid and biochemical experiments suggested that Scrib and TMIGD1 interact directly through the Scrib PDZ1 domain and the PBM of TMIGD1. We examined the structural basis of this putative binding interface by determining the crystal structure of the isolated Scrib PDZ1 domain in complex with an 8-mer peptide representing the C-terminal region of TMIGD1 including the PBM (-DPHSETAL$_{COOH}$, PBM underlined). The PDZ1:TMIGD1 structure was refined to a resolution of 1.9 Å with a final R_{free} of 0.222 (Table S1). As shown previously, the Scrib PDZ1 domain adopts a compact globular fold comprising six β-strands and two α-helices that adopt a β-sandwich structure [29], a conformation that is typical for PDZ domains [30]. The TMIGD1 peptide engaged with the PDZ1 domain via the well-conserved canonical ligand binding groove located between the β2 strand and the α2 helix (Fig. 3A) [29, 31, 32, 33, 34]. Binding of TMIGD1 to Scrib PDZ1 does not alter the overall domain configuration of Scrib PDZ as a superimposition of ligand-free Scrib PDZ1 with the Scrib PDZ1:TMIGD1 yielded a root-mean-square deviation of 0.44 Å, with differences between the two structures primarily due to changes in local side chain conformations.

Close examination of Scrib PDZ1:TMIGD1 peptide complex revealed several direct interactions that are formed between the peptide and the PDZ1 domain (Fig. 3B, Fig. S1). The C-terminal carboxyl group of the TMIGD1 peptide docks in the conserved hydrophobic pocket of PDZ1, interacting with the main chain L736^{PDZ1}, G737^{PDZ1} and I738^{PDZ1}. Furthermore, a network of hydrogen bonds is observed between the PDZ1 and the TMIGD1 peptide, including interactions of I740^{PDZ1}:A261^{TMIGD1}, I740^{PDZ1}:T260^{TMIGD1}, H791^{PDZ1}:T260^{TMIGD1}, T747^{PDZ1}:D255^{TMIGD1} and T747^{PDZ1}: P256^{TMIGD1}. Lastly, a salt bridge is found between R760^{PDZ1} and E259^{TMIGD1}.

Scribble interacts with TMIGD1 through PDZ1 and PDZ3 domains

Given the extensive interaction network of Scrib [15, 17, 35] we aimed to characterize the Scrib – TMIGD1 interaction in more detail. To address the possibility that Scrib interacts with TMIGD1 through additional PDZ domains, we performed *in vitro* binding assays using the cytoplasmic domain of TMIGD1 fused to GST and *in vitro* translated Scrib PDZ domain constructs in which individual PDZ domains were inactivated by mutating the GLGF motif [36] (Fig. 4A). Mutating PDZ1 strongly reduced binding to TMIGD1, as expected (Fig. 4B). Mutating PDZ2 and PDZ3 also strongly reduced the binding to TMIGD1 suggesting that PDZ2 and PDZ3 are also involved in the interaction with TMIGD1. Mutating PDZ4 did not reduce the binding to TMIGD1 (Fig. 4B). These observations thus indicated that Scrib interacts with TMIGD1 not only through PDZ1 but also through PDZ2 and PDZ3. Direct interactions of Scrib with the same ligand through several of its PDZ domains have been observed for many other Scrib ligands [15, 17], which highlights Scrib's role as a multifunctional scaffold for the assembly of diverse multiprotein complexes.

Overlapping preferences of the Scrib PDZ domains against the same ligand can be fine-tuned by different mechanisms including differential affinities [15]. To understand how PDZ1, PDZ2 and PDZ3 of Scrib contribute to the interaction with TMIGD1 we examined the affinities of the 8-mer peptide representing the TMIGD1 C-terminus towards the four individual recombinant PDZ domains by isothermal titration calorimetry (ITC). A similar peptide with mutations at positions 0 and -2, which classify the TMIGD1 PBM as Class I [37] (-DPHSEAAA$_{COOH}$), was used as control. We observed affinities of 18.17 µM and 9.12 µM for PDZ1 and PDZ3, respectively (Table 1, Table S2). These findings indicated that both PDZ1 and PDZ3 autonomously bind TMIGD1, and that TMIGD1 binds to Scrib PDZ3 with a two-fold higher affinity than it binds PDZ1 (Fig. 4C, Table 1). Surprisingly, despite the strong reduction in TMIGD1 binding affinity when PDZ2 is mutated (Scrib/PDZ2-mut) (Fig. 4B), the recombinant PDZ2 alone did not bind TMIGD1 (Fig. 4C, Table 1). PDZ4 did not show any affinity towards TMIGD1 (Fig. 4C, Table 1). None of the four Scrib PDZ domains interacted with the control peptide (Table 1). These observations identified PDZ1 and PDZ3 as the PDZ domains of Scrib that directly interact with TMIGD1, and they established a hierarchy between these two PDZ domains. The finding that the isolated PDZ2 does not bind to TMIGD1 whereas the PDZ2 mutant in the context of the Scrib/PDZ domain construct impairs binding to TMIGD1 suggests that PDZ2 binding to TMIGD1 may be regulated by cooperative activities of regions outside PDZ2, as described for Scrib PDZ interactions with other ligands including the α_{1D}-adrenergic receptor [38, 39].

Table 1: Comparison of ITC data obtained from WT and mutant TMIGD1 peptides. Each of the values was calculated from at least three independent experiments.

TMIGD1 Peptides	Sequence	Scrib-PDZ1	Scrib-PDZ2	Scrib-PDZ3	Scrib-PDZ4
TMIGD1/WT	DPHSETAL	18.17 ± 1.80 µM	NB	9.12 ± 0.670 µM	NB
TMIGD1/mut	DPHSEAAA	NB	NB	NB	NB

TMIGD1 recruits Scribble to cell-cell contacts

Our observations of a direct PDZ domain-mediated interaction of Scrib with TMIGD1 identified TMIGD1 as the first cell-cell adhesion receptor of epithelial cells with the ability to directly interact with Scrib. To test if TMIGD1 recruits Scrib to the basolateral membrane, we ectopically expressed myc-tagged Scrib constructs (depicted in Fig. 2A) in HEK293 cells stably transfected with TMIGD1/WT or TMIGD1/Δ5. Scrib full length localized to cell-cell contacts irrespective of the presence of TMIGD1/WT or TMIGD1/Δ5 (Fig. 5A), suggesting TMIGD1-independent recruitment mechanisms for Scrib, which is consistent with observations of multiple potential binding partners for Scrib [17]. The Scrib/LRR construct was exclusively localized in the cytoplasm (Fig. 5A, B), indicating that PDZ domains are necessary for membrane localization of Scrib. The Scrib/PDZ construct was localized in the cytoplasm of wildtype HEK293 cells, but was strongly recruited to cell-cell contacts in TMIGD1/WT-expressing cells in a manner that depended on the PBM of TMIGD1 (Fig. 5A, B). These findings indicated that in the absence of the LRR region, which

contains the Pro305 residue critical for membrane localization [18], TMIGD1 recruits Scrib to cell-cell junctions through a PDZ domain interaction. Notably, in HEK293 cells expressing the Scrib PDZ domain construct with a C-terminal CAAX motif (Scrib/PDZ-CAAX), which targets proteins to endomembranes such as the ER and the Golgi [40], TMIGD1 was enriched at endomembrane compartments (Fig. 5C). These findings identified TMIGD1 as a cell adhesion receptor which recruits Scrib to cell-cell contacts in epithelial cells. They also indicated that TMIGD1 and Scrib can influence each other's localization in a mutual manner, a property that may have an impact on the tumor-suppressing properties of these two proteins.

Dominant-negative TMIGD1 impairs apical-basal polarity in MDCKII cells

Our observations on the interaction of TMIGD1 with Scrib as a regulator of cell polarity and as a tumor suppressor protein suggested a possible role of TMIGD1 in the regulation of apical-basal cell polarity. To test this, we used MDCK cells, which are polarized epithelial cells derived from kidney distal tubules [41]. When grown in a three-dimensional matrix of collagen I or matrigel, MDCK cells develop into spheroids consisting of a lumen surrounded by a single layer of epithelial cells. Individual cells are polarized along the apical-basal polarity axis with an apical domain facing the lumen, a lateral domain in contact with adjacent cells, and a basal domain in contact with the ECM [42]. A failure in developing apical-basal polarity, for example after inhibition of cell polarity proteins CRB3, PATJ, PAR3 or aPKC, results in the development of multicellular aggregates instead of single lumen-containing cysts [43, 44, 45, 46, 47]. To test a role of TMIGD1 in cystogenesis we ectopically expressed a TMIGD1 mutant that lacked the membrane-distal Ig-like domain. Previous studies had shown that an analogous mutant of the TMIGD1-related Ig-SF family member JAM-A acts in a dominant-negative manner in the development of apical-basal polarity and cyst formation [48, 49]. Control MDCKII cells developed normal cysts containing a single lumen surrounded by single-layered epithelium (Fig. 6). Induced expression of ΔD1/TMIGD1 impaired the formation of single lumen-containing cysts and resulted in the formation of multicellular aggregates without lumen (Fig. 6A, B), a phenotype which strongly resembles the phenotype observed after depletion of Scrib in mammary gland-derived acinar epithelial cells [50] and in lung organotypic cultures [51]. Multilumenal cysts, which can also be observed after interfering with the function of polarity proteins [52, 53, 54], were not observed in ΔD1/TMIGD1-expressing cells (Fig. 6B). These observations suggest a role for TMIGD1 in the development of apical-basal polarity in polarized epithelial cells.

Discussion

In this study we identify the cell adhesion molecule TMIGD1 as membrane anchor for the Scrib tumor suppressor protein. TMIGD1 and Scrib interact directly through a PDZ domain-mediated interaction that involves three out of the four Scrib PDZ domains. Importantly, after inactivating the endogenous mechanism of Scrib membrane recruitment – by deleting the Scrib LRR domain – Scrib recruitment to the membrane depends on TMIGD1. Our findings thus identify a mechanism of Scrib membrane recruitment that depends on its PDZ domain region and that operates in addition to the LRR domain-dependent

mechanism of membrane recruitment. Our findings also identify TMIGD1 as an adhesion receptor localized at cell-cell contacts of polarized epithelial cells which recruits Scrib to the lateral membrane domain. Given that the tumor-suppressive activity of Scrib strongly depends on its membrane localization [16], these findings have important implications for tumor development.

Despite a strong interaction between recombinant TMGID1 and Scrib constructs (Figs. 1B, 4B), the interaction between the full-length proteins expressed in cells was relatively weak (Fig. 1C). We explain this observation by the fact that Scrib can interact with a large number of interaction partners (summarized in refs [15, 17]. At least 37 proteins directly interact with the PDZ domains of Scrib, and in the majority of cases, i.e. 25, these interactions involve more than one PDZ domain [17]. It is very likely that some of these binding partners interact with one or more Scrib PDZ domains with higher affinities than TMIGD1, thus outcompeting TMIGD1 from Scrib binding. For example, the affinity of the adenomatous polyposis coli (APC) PBM peptide for Scrib PDZ1 is approximately three-fold higher than that of the TMIGD1 PBM peptide (K_D = 6.0 μM vs K_D = 18.17 μM for APC vs TMIGD1, respectively [32], suggesting that APC binding to Scrib PDZ1 will be favored over TMIGD1 binding. Another possibility to explain the weak interaction of TMIGD1 and Scrib in cells is that ligands which interact with Scrib could favor a conformation of Scrib that is unfavorable to TMIGD1 binding.

We have also observed that the recombinant PDZ2 domain of Scrib had no affinity towards the TMIGD1 C-terminal peptide (Fig. 4C). On the other hand, inactivation of PDZ2 in a Scrib/PDZ1-4 construct resulted in a strong reduction in TMIGD1 binding in GST-pulldown assays (Fig. 4B), which suggested that PDZ2 contributes to TMIGD1 binding (Fig. 4B). These observations could be explained by a co-operative mechanism between the Scrib PDZ domains. Examples for such co-operative binding mechanisms exist. The α_{1D}-adrenergic receptor interacts with Scrib PDZ domains in a way such that binding of the α_{1D}-adrenergic to one PDZ domain of Scrib strongly enhances its binding to the other PDZ domains [38]. Since GST-fusion proteins dimerize through the GST-domain [55], dimerized GST-TMIGD1 fusion proteins could thus bind two different PDZ domains within the Scrib/PDZ1-4 construct. Co-operative interactions between PDZ1 or PDZ3 with PDZ2 of Scrib could thus promote the interaction of Scrib PDZ2 with TMIGD1.

Despite its physiological and, in particular, pathophysiological relevance, the mechanisms of Scrib membrane targeting are not well understood. Anchoring at the lateral membrane domain of epithelial cells depends on the LRR-region [56, 57, 58]. Mutating Pro305 in the LRR12 to Leu (Scrib/P305L) abolishes membrane localization [50, 58, 59, 60]. Thus, the LRR region of Scrib is a dominant driver of Scrib membrane localization. Importantly, ectopic expression of Scrib/P305L in cell lines disrupts cell polarity, suppresses c-myc-induced apoptosis, enhances Akt signaling, and fails to suppress Ras-MAPK-induced EMT [18, 50, 59, 61]. Also, transgenic mice expressing Scrib/P305L in the mammary gland display hyperplastic growth in the mammary gland and develop mammary tumors [18]. These findings indicated that the function of Scrib as tumor suppressor depends on membrane localization, and that the LRR domain of Scrib is the dominant force for membrane localization.

Previous studies in Drosophila and in vertebrate MDCK cells, however, showed that Scrib constructs lacking the entire LRR region can also localize to cell-cell junctions [57, 58, 62], raising the question why the Scrib/P305L is not recruited by a PDZ domain-dependent mechanism. It is possible that replacing Pro305 with a hydrophobic Leu residue alters the conformation of the horseshoe-like structure of the LRR domain [63], which could abolish LRR-mediated interactions required for membrane recruitment [64], enhance interactions with a cytoplasmic protein, as demonstrated for ZDHHC7 [60], or mask the PDZ domains of Scrib making these inaccessible for the many PDZ domain-dependent interaction partners [17]. Another possibility would be that the P305 mutation abolishes homodimerization, which is mediated through the LRR region [64], and that homodimerization is required for membrane tageting.

A role of TMIGD1 in recruiting Scrib to the lateral membrane is consistent with a predicted function of TMIGD1 as tumor suppressor protein. Several unbiased studies describe a strong and highly significant reduction of TMIGD1 gene expression in colon cancer in humans [65, 66, 67, 68] with a progressive downregulation during disease progression [20, 69]. Also, several studies found a significant downregulation of TMIGD1 gene expression in diseases associated with chronic intestinal inflammation such as Crohn's disease or inflammatory bowel disease [24, 66, 70], conditions which promote carcinogenesis [71]. In further support of a role of TMIGD1 as tumor suppressor, inactivation of the *Tmigd1* gene in mice results in a grossly altered morphology of intestinal tissues associated with intestinal adenoma formation and enhanced proliferative activity in intestinal crypts [25]. Finally, TMIGD1 expression has also been found to be downregulated in kidney cancer [22]. Together, these findings support the hypothesis that the function of TMIGD1 as tumor suppressor is linked to its ability to recruit Scrib to the membrane. It will thus be important to study a cause-and-effect relationship between loss of TMIGD1 expression and Scrib mislocalization during cancer development.

Methods

Cell culture and transfections

HEK293T cells (ATCC-CRL-2316) were grown in DMEM containing 10% FCS, 1% NEAA, 2 mM L-Glu, 100 U/ml Pen/Strep. Stably transfected HEK293 cells expressing TMIGD1/WT or TMIGD1/Δ5 were generated by electroporation (0.25 kV, 950 µF) and cultured in growth media supplemented with G418 (800 µg/ml). Positive clones were identified by Western blot analysis and immunofluorescence microscopy. Transient transfections of cDNAs were performed using Lipofectamine 2000 (ThermoFisher Scientific, #11668-019) and X-Fect (Xfect™ Transfection Reagent, TakaraBio-Clontech #631318), according to manufacturer's instructions. MDCK II Tet-Off cell lines (TakaraBio-Clontech, St-Germain-en-Laye, # 630913/631138) were maintained in DMEM containing 10% FCS, 2 mM L-glutamine, 100 U/ml Pen/Strep, 100 µg/ml G418 and 1 µg/ml puromycin. MDCK II Tet-Off cells stably expressing a human TMIGD1 mutant lacking the membrane-distal Ig-domain (ΔD1-TMIGD1) were generated by electroporation and subsequent selection by growth in DMEM medium supplemented with 150 µg/ml hygromycin and 50 ng/ml doxycycline (Dox). Expression of transgenes was induced by transferring cells into medium lacking Dox using tetracycline-

free FCS (BD Biosciences) [23]. All cell lines were routinely tested and found to be negative for mycoplasma contamination.

Expression vectors

The following constructs were used. TMIGD1 constructs in pcDNA3 (Invitrogen): hTMIGD1 full length (AA1-262), hTMIGD1 lacking the PDZ domain binding motif (hTMIGD1/Δ5, AA 1-258). TMIGD1 constructs in pKE576hyg: Flag-tagged human TMIGD1 lacking the membrane-distal Ig-like domain (hΔD1/TMIGD1, AA 115 - 262) [23]. GST-tagged TMIGD1 constructs in pGEX-4T-1 (GE Healthcare): GST-TMIGD1 (hTMIGD1 cytoplasmic tail (AA 242-262); GST-TMIGD1/Δ5: hTMIGD1 cytoplasmic tail lacking the PDZ domain binding motif (AA 242-257). TMIGD1 constructs in yeast-two hybrid vector pBTM116 [72]: pBTM116-TMIGD1 (cytoplasmic tail of hTMIGD1, AA 241-262). TMIGD1-Fc fusion constructs in pcDNA3-hIgG: hTMIGD1-Fc (extracellular domain of hTMIGD1, AA 1 - 222).

Human Scribble (Uniprot accession number Q14160) constructs in pcDNA3:His/Xpress [36]: hScrib/PDZ-WT (AA 616-1490), hScrib/PDZ-mut1 (AA 616-1490_$L_{738}AG_{739}E$), hScrib/PDZ-mut2 (AA 616-1490_$L_{872}AG_{873}E$), hScrib/PDZ-mut3 (AA 616-1490_$L_{1014}AG_{1015}E$), hScrib/PDZ-mut4 (AA 616-1490_$L_{1111}AG_{1112}E$). Human Scrib constructs in pKE081myc (N-terminal myc tag, [73]: hScrib/WT (AA 2-1630), hScrib/LRR (AA 2-727), hScrib/PDZ (AA 665-1630), hScrib/PDZ-CAAX (AA 665-1630 with C-terminal CAAX box (GCMSCKCVLS) derived from H-Ras). Human Scrib PDZ domain constructs in pGEX-6P-3 (GE Healthcare) or pGIL-MBP [74]: hScrib/PDZ1 (AA 728-815), hScrib/PDZ2 (AA 833-965), hScrib/PDZ3 (AA 1005-1094), hScrib/PDZ4 (AA 1099-1203). Erbin constructs in pEGFP-GW (kindly provided by Dr. Jean-Paul Borg, Inserm, CNRS, Marseille, France): hErbin/WT (AA 1-1412). Lano constructs in pcDNA-HA (kindly provided by Dr. Jean-Paul Borg, Inserm, CNRS, Marseille, France): hLano/WT (AA 1 – 524).

Antibodies and reagents

The following antibodies were used in this study: rabbit pAb anti-TMIGD1 (SA #HPA021946, IF 1:500); mouse mAb anti-α-Tubulin (SA, clone B-5-1-2, #T5168, IF 1:500, WB 1:10.000); goat pAb anti-Myc (SantaCruz #sc-789G, IF 1:500, WB 1:500); mouse mAb anti-Myc 9E10 [75] (IF 1:500, WB 1:500); mouse mAb anti-GFP (Takara #632375, WB 1:500); rabbit pAb anti-Hemagglutinin (HA) (SA, #H6908, WB: 1:500); rabbit pAb anti-Flag (SA, #F7425, IF 1:500). Rabbit anti-TMIGD1 pAb Affi1662/1663 was generated by immunizing rabbits with a fusion protein consisting of the extracellular domain of hTMIGD1 fused to the Fc region of human IgG, as described previously [26] (IF 1:500, WB 1:500). The antibodies were affinity-purified by adsorption at the antigen covalently coupled to cyanogen bromide (CNBr)-activated sepharose beads (Amersham Biosciences Europe, Freiburg, Germany). Antibodies directed against the Fc part were depleted by adsorption at human IgG coupled to CNBr-activated sepharose beads. Affinity-purified antibodies were dialyzed against PBS. Secondary antibodies and fluorophore-conjugated antibodies: Fluorophore-conjugated antibodies for Western blotting: IRDye 800CW Donkey anti-Rabbit IgG (LI-COR Biosciences #926-32213, WB 1:10.000), IRDye 680CW Donkey anti-mouse IgG (LI-COR Biosciences #926-

68072, WB 1:10.000). Fluorophore-conjugated secondary antibodies for ICC: Donkey anti-Mouse IgG (H+L) Alexa Fluor 594 (ThermoFisher Scientific #A-21203); Donkey anti-Rabbit IgG (H+L) Alexa Fluor 594 (ThermoFisher Scientific #A-21207); Donkey anti-Rabbit IgG(H+L) Alexa Fluor 488 (ThermoFisher Scientific #A-21206); Donkey anti-Mouse IgG (H+L) Alexa Fluor 488 (Dianova/Jackson ImmunoResearch Europe Ltd #715-545-150); Donkey anti-Mouse IgG (H+L) Alexa Fluor 647 (Dianova/Jackson ImmunoResearch Europe Ltd #715-605-150) -conjugated, highly cross-adsorbed secondary antibodies (all Alexa Fluor-conjugated secondary antibodies for IF were used in a dilution of 1:800). The following peptides were used for crystallization and ITC: -DPHSETAL, -DPHSEAAA; peptides were obtained from Genscript. The following reagents were used: Dox (SA #D9891), collagen type I (rat tail type 1 collagen, Advanced BioMatrix #5163), 2,4,diamidino-2-phenylindole (DAPI, SA # D9542).

Yeast Two-hybrid Screen

Yeast two-hybrid screening experiments were performed essentially as described [73]. Briefly, the Saccharomyces cerevisiae reporter strain L40 expressing a fusion protein between LexA and the cytoplasmic tail of TMIGD1 (AA 241–262) was transformed with 250 µg of DNA derived from a day 9.5/10.5 mouse embryo cDNA library [27] according to the method of Schiestl and Gietz [76]. The transformants were grown for 16 h in liquid selective medium lacking tryptophan, leucine (SD-TL) to maintain selection for the bait and the library plasmid, then plated onto synthetic medium lacking tryptophan, histidine, uracil, leucine, and lysine (SD-THULL) in the presence of 1 mM 3-aminotriazole. After 3 days at 30 °C, large colonies were picked and grown for an additional three days on the same selective medium. Plasmid DNA was isolated from growing colonies using a commercial yeast plasmid isolation kit (DualsystemsBiotech, Schlieren, Switzerland). To segregate the bait plasmid from the library plasmid, yeast DNA was transformed into E. coli HB101, and the transformants were grown on M9 minimal medium lacking leucine. Plasmid DNA was then isolated from E. coli HB101 followed by sequencing to determine the nucleotide sequence of the inserts.

Immunoprecipitation and Western blot analysis

For immunoprecipitations (IPs), cells were lysed in lysis buffer (25 mM TrisHCl, pH 7.4, 1% (v/v) Nonidet P-40 (NP-40, AppliChem, Darmstadt, Germany), 150 mM NaCl, protease inhibitors (Complete Protease Inhibitor Cocktail; Roche, Indianapolis, IN), 5% glycerol (AppliChem #A2926) and phosphatase inhibitors (PhosSTOP^{TM}, Roche, Indianapolis, IN), 2 mM sodium orthovanadate) for 20 min with overhead rotation at 4°C followed by centrifugation (15.000 rpm, 20 min at 4°C). Postnuclear supernatants were incubated with 3 µg of antibodies coupled to protein A– or protein G–Sepharose beads (GE Healthcare, Solingen, Germany) for 4 h at 4°C. Beads were washed five times with lysis buffer, bound proteins were eluted by boiling in 3x SDS-sample buffer/150 mM DTT. Eluted proteins were separated by SDS–PAGE and analyzed by Western blotting with near-infrared fluorescence detection (Odyssey Infrared Imaging System Application Software Version 3.0 and IRDye 800CW-conjugated antibodies; LI-COR Biosciences, Bad Homburg, Germany). All IP and Western blot experiments shown in this study are representative for at least three independent experiments.

Protein expression and purification of recombinant Scrib PDZ constructs

All proteins were overexpressed in *E. coli* BL21 (DE3) CodonPlus or *E. coli* BL21 (DE3) pLysS cells (BIOLINE) via manual induction using 0.5 mM isopropyl 1-thio-b-d-galactopyranoside either as Glutathione S-transferase or Maltose Binding Protein fusions. Recombinant protein purification and tagged protein cleavage were carried out as described previously [29]. Purified Scribble PDZ domains were subsequently dialysed into 25 mM Tris-HCl pH 8.0, 150 mM NaCl, 5 mM TCEP (Tris(2-carboxyethyl) phosphine hydrochloride (Buffer A) for downstream applications.

GST pulldown experiments

In vitro binding experiments were performed with recombinant GST-TMIGD1 fusion proteins purified from *E.coli* and immobilized on glutathione-Sepharose 4B beads (Life Technologies #17-0756-01). Purification of GST fusion proteins was performed as described [73]. For the analysis of direct protein interactions, Scrib constructs were translated in vitro using the TNT T7-coupled reticulocyte lysate system (Promega Corp., Madison, WI) in the presence of ^{35}[S]-labeled methionine (Hartmann Analytic GmbH, Braunschweig, Germany) as described by the manufacturer. 10 µl of the translation reactions were incubated with 3 µg of immobilized GST fusion protein for 2 h at 4°C under constant agitation in buffer B (10 mM Hepes-NaOH (pH7.4), 100 mM KCl, 1 mM $MgCl_2$, 0.1% Triton X-100). After 5 washing steps in buffer B bound proteins were eluted by boiling for 5 min in SDS sample buffer, subjected to SDS-PAGE and analyzed by fluorography. All in vitro binding experiments shown in this study are representative for at least three independent experiments.

MDCK II cyst assays

MDCK cyst assays were performed essentially as described [48, 77] . Briefly, MDCK II cells were seeded as single cell suspension (3.4×10^4 cells/ml) in 0.18% type I collagen from rat tail (BD Biosciences). After 3-6 d, the gels were washed in PBS, subjected to collagenase treatment (100 U/ml collagenase VII (Sigma), 15 min, RT) and fixed (4% paraformaldehyde/PBS, 30 min, RT). Cells were permeabilized by treatment with 0.25% Triton X-100/PBS (30 min, RT) and washed extensively with 2% goat serum/PBS (1 h, RT). Incubations with primary and fluorochrome-conjugated secondary antibodies were performed in 2% goat serum/PBS for a minimum of 12 h at 4°C. After extensive washing, the gels were mounted on glass coverslips using Kaiser's glycerol gelatine (Merck, Darmstadt, Germany). Cysts were analyzed using a confocal microscope as specified in the Immunocytochemistry and Immunofluorescence microscopy paragraph.

Immunocytochemistry and immunofluorescence microscopy

For immunofluorescence microscopy, cells were grown on collagen-coated glass slides. Cells were washed with PBS and fixed with 4% paraformaldehyde (PFA, Sigma-Aldrich) for 7 min or with -20°C-cold MeOH for 5 min. To detect intracellular proteins, PFA-fixed cells were incubated with PBS containing 0.2% Triton X-100 for 15 min. Cells were washed with 100 mM glycine in PBS, blocked for 1h in blocking buffer

(PBS, 10% FCS, 0.2% Triton X-100, 0.05% Tween-20, 0.02% BSA) and then incubated with primary antibodies in blocking buffer for 1 h at room temperature (RT) or overnight at 4°C. After incubation, cells were washed three times with PBS and incubated with fluorochrome (AlexaFluor488, AlexaFluor594 and AlexaFluor647)-conjugated, highly cross-adsorbed secondary antibodies (Invitrogen) for 2 hrs at RT protected from light. F-Actin was stained using phalloidin-conjugates (TRITC and cytoPainter iFluor-647, DNA was stained with 4,6-diamidino-2-phenylindole (DAPI, SA). Samples were washed three times with PBS and mounted in fluorescence mounting medium (Mowiol 4-88, SA). Immunofluorescence microscopy was performed using the confocal microscope LSM 800 Airyscan (Carl Zeiss, Jena, Germany) equipped with the objective Plan-Apochromat x 63/1.4 oil differential interference contrast (Carl Zeiss). Image processing and quantification was performed using ImageJ and Zen 2 (Blue Edition, Carl Zeiss) softwares. For quantification of Scrib recruitment to the lateral membrane domain by TMIGD1, at least 60 and maximally 90 cells per condition (derived from 3 independent experiments) were analyzed. Statistical analysis was performed using unpaired Student`s t test, data is plotted as means ± standard deviation (SD). P-values: *P<0.05, ****P<0.001.

Isothermal titration calorimetry

All titration experiments were performed with the purified PDZ domains in Buffer A against C-terminally derived 8-mer human TMIGD1 peptide (DPHSETAL; UniProt ID: Q6UXZ0) and a mutant TMIGD1 peptide with the sequence DPHSEAAA. Protein concentrations were measured using a NanoDrop 2000 spectrophotometer (Thermo Fisher scientific) as described previously [33, 78]. Each domain was used at a concentration of 75 µM and the peptide concentration was 900-1100 µM. Titrations were performed at 25°C with a stirring speed of 750 rpm using the Microcal™ NanoITC200 system (GE Healthcare) with a total of 20 injections. Raw data was processed with MicroCal Origin version 7.0 software (OriginLabTM Corporation) using a one-site binding model. The affinity data of each protein were compared to the positive control of a synthetic pan-PDZ binding peptide known as super peptide (RSWFETWV) [79].

Protein crystallization

Scrib/PDZ1:TMIGD1 PBM peptide complexes were prepared for crystallisation trials as described previously [80]. The protein:peptide complexes were resuspended in buffer A at a molar ratio of 1:4. Using an in-house Gryphon LCP liquid dispenser (Art Robbins Instruments), initial sparse matrix crystallisation trials were performed in 96-well sitting drop trays (Swissci AG, Neuheim, Switzerland) with 0.2 µl of protein sample and 0.2 µl reservoir per drop. Subsequent crystal optimisations were carried out in 24-well Limbro plates (Hampton Research). All crystallisation trials were performed at 20°C. Human Scribble PDZ1:Human TMIGD1 PBM crystals were obtained at 8 mg/ml in 24% w/v PEG 1500, flashed cool in 20% ethylene glycol.

Diffraction data collection and structure determination

All diffraction data were collected on the MX2 beamline at the Australian Synchrotron using an Eiger detector (Dectris, Baden-Dättwil, Switzerland) with an oscillation range of 0.1° per frame using a

wavelength of 0.9537 Å. Diffraction data was integrated using DIALS and scaled with AIMLESS [81, 82, 83]. The structure of Scribble/PDZ1:TMIGD1 peptide complex was solved by molecular replacement with Phaser using human Scribble PDZ1:human APC (PDB ID: 6XA8) [34] as the search model [84]. The molecular replacement solution was manually rebuilt using Coot and refined with PHENIX [85, 86]. Data collection and refinement statistics are summarised in Table S1. Final images of Scrib/PDZ1:TMIGD1 peptide complex were generated using the PyMOL molecular graphic system, version 1.8.6 (Schrödinger, LLC, New York, USA) and all software was accessed through SBGrid suite [87]. All raw diffraction images were deposited on the SBGrid Data Bank [88] using the PDB accession code XXX.

Statistics and reproducibility

Results are expressed either as arithmetic means ± SD as indicated. To test the normality of data sample distributions, the D'Agostino-Pearson normality test was used. Data were statistically compared using unpaired, two-tailed Student's *t*-test, or probed for being statistically different from a fixed value using One sample *t*-test. Statistical analyses were performed using GraphPad Prism version 6 (GraphPad Software, San Diego, CA). P-values are indicated as follows: *P<0.05, **P<0.01, ***P<0.001 and ****P<0.0001. For each statistical analysis data derived from at least three independent experiments were used. Experiments were considered independent when they reflected biological replicates acc. to [89]. Sample sizes are indicated for all experiments in the respective figure legends.

Abbreviations

CoIP, co-immunoprecipitation; TMIGD1, Transmembrane and immunoglobulin domain-containing protein 1; Scrib, Scribble

AA, amino acid, IF, immunofluorescence; PBM, PDZ domain-binding motif; PDZ, Postsynaptic density 95 - Discs Large - Zonula occludens-1; Scrib, Scribble; TMIGD1, Transmembrane and immunoglobulin domain-containing protein 1.

Declarations

Acknowledgements

We gratefully acknowledge the help of Dr. Jean-Paul Borg (Centre der Recherche en Cancérolgie de Marseille, Aix Marseille University, Inserm, CNRS, Marseille, France) who provided us with expression vectors encoding Erbin and Lano/LRRC1. We also thank Frauke Brinkmann for excellent technical assistance. We thank the staff at the MX beamlines at the Australian Synchrotron for help with X-ray data collection, and the Comprehensive Proteomics Platform at La Trobe University for core instrument support. We thank the ACRF for supporting the Eiger MX detector at the Australian Synchrotron MX2 beamline.

Ethics approval

NA

Author contributions

E.-M.T., C.H., M.K., P.O.H., and K.E. designed and conceived the study. E.-M.T., C.H., J.C.M. A.J. and B.E.M. performed experiments. L.B. provided reagents. E.-M.T., C.H., V.G., M.K., P.O.H. and K.E. analyzed the data. E.-M.T. M.K., P.O.H. and K.E. wrote the manuscript.

Competing interests

The authors declare that they have no competing interest.

Data availability

Data supporting the findings of this manuscript are available from the corresponding authors upon reasonable request.

Funding

This work was supported by grants from the Deutsche Forschungsgemeinschaft (EB 160/8-1; EXC 1003-CiMIC) to KE, the National Health and Medical Research Council Australia (Project Grant APP1103871 to MK, POH; Senior Research Fellowship APP1079133 to POH) and La Trobe University (Research focus area “Understanding Disease” project grant and scholarship to JCM and AJ.

References

1. Buckley CE, St Johnston D. Apical-basal polarity and the control of epithelial form and function. *Nat Rev Mol Cell Biol*, (2022).
2. Buchheit CL, Weigel KJ, Schafer ZT. Cancer cell survival during detachment from the ECM: multiple barriers to tumour progression. *Nat Rev Cancer* **14**, 632-641 (2014).
3. Thiery JP, Sleeman JP. Complex networks orchestrate epithelial-mesenchymal transitions. *Nat Rev Mol Cell Biol* **7**, 131-142 (2006).
4. Polyak K, Weinberg RA. Transitions between epithelial and mesenchymal states: acquisition of malignant and stem cell traits. *Nat Rev Cancer* **9**, 265-273 (2009).
5. Pei D, Shu X, Gassama-Diagne A, Thiery JP. Mesenchymal-epithelial transition in development and reprogramming. *Nature cell biology* **21**, 44-53 (2019).
6. Lambert AW, Weinberg RA. Linking EMT programmes to normal and neoplastic epithelial stem cells. *Nat Rev Cancer* **21**, 325-338 (2021).
7. Macara IG. Parsing the polarity code. *Nat Rev Mol Cell Biol* **5**, 220-231 (2004).
8. Ebnet K, Gerke V. Rho and Rab Family Small GTPases in the Regulation of Membrane Polarity in Epithelial Cells. *Front Cell Dev Biol* **10**, 948013 (2022).

9. Tan B, Yatim S, Peng S, Gunaratne J, Hunziker W, Ludwig A. The Mammalian Crumbs Complex Defines a Distinct Polarity Domain Apical of Epithelial Tight Junctions. *Curr Biol* **30**, 2791-2804 e2796 (2020).
10. Morais-de-Sa E, Mirouse V, St Johnston D. aPKC phosphorylation of Bazooka defines the apical/lateral border in Drosophila epithelial cells. *Cell* **141**, 509-523 (2010).
11. Zihni C*, et al.* Dbl3 drives Cdc42 signaling at the apical margin to regulate junction position and apical differentiation. *J Cell Biol* **204**, 111-127 (2014).
12. Benton R, St Johnston D. Drosophila PAR-1 and 14-3-3 inhibit Bazooka/PAR-3 to establish complementary cortical domains in polarized cells. *Cell* **115**, 691-704 (2003).
13. Halaoui R, McCaffrey L. Rewiring cell polarity signaling in cancer. *Oncogene* **34**, 939-950 (2015).
14. Fomicheva M, Tross EM, Macara IG. Polarity proteins in oncogenesis. *Curr Opin Cell Biol* **62**, 26-30 (2020).
15. Stephens R, Lim K, Portela M, Kvansakul M, Humbert PO, Richardson HE. The Scribble Cell Polarity Module in the Regulation of Cell Signaling in Tissue Development and Tumorigenesis. *J Mol Biol* **430**, 3585-3612 (2018).
16. Santoni MJ, Kashyap R, Camoin L, Borg JP. The Scribble family in cancer: twentieth anniversary. *Oncogene* **39**, 7019-7033 (2020).
17. Bonello TT, Peifer M. Scribble: A master scaffold in polarity, adhesion, synaptogenesis, and proliferation. *J Cell Biol* **218**, 742-756 (2019).
18. Feigin ME*, et al.* Mislocalization of the cell polarity protein scribble promotes mammary tumorigenesis and is associated with Basal breast cancer. *Cancer research* **74**, 3180-3194 (2014).
19. Zhao D, Yin Z, Soellner MB, Martin BR. Scribble sub-cellular localization modulates recruitment of YES1 to regulate YAP1 phosphorylation. *Cell Chem Biol* **28**, 1235-1241 e1235 (2021).
20. Cattaneo E*, et al.* Preinvasive colorectal lesion transcriptomes correlate with endoscopic morphology (polypoid vs. nonpolypoid). *EMBO molecular medicine* **3**, 334-347 (2011).
21. Arafa E*, et al.* TMIGD1 is a novel adhesion molecule that protects epithelial cells from oxidative cell injury. *The American journal of pathology* **185**, 2757-2767 (2015).
22. Meyer RD*, et al.* TMIGD1 acts as a tumor suppressor through regulation of p21Cip1/p27Kip1 in renal cancer. *Oncotarget* **9**, 9672-9684 (2018).
23. Hartmann C*, et al.* The mitochondrial outer membrane protein SYNJ2BP interacts with the cell adhesion molecule TMIGD1 and can recruit it to mitochondria. *BMC Mol Cell Biol* **21**, 30 (2020).
24. Zabana Y*, et al.* Transcriptomic identification of TMIGD1 and its relationship with the ileal epithelial cell differentiation in Crohn's disease. *American journal of physiology* **319**, G109-G120 (2020).
25. De La Cena KOC*, et al.* Transmembrane and Immunoglobulin Domain Containing 1, a Putative Tumor Suppressor, Induces G2/M Cell Cycle Checkpoint Arrest in Colon Cancer Cells. *The American journal of pathology* **191**, 157-167 (2021).

26. Hartmann C*, et al.* Intestinal brush border formation requires a TMIGD1-based intermicrovillar adhesion complex. *Science signaling* **15**, eabm2449 (2022).
27. Hollenberg SM, Sternglanz R, Cheng PF, Weintraub H. Identification of a new family of tissue-specific basic helix-loop-helix proteins with a two-hybrid system. *Mol Cell Biol* **15**, 3813-3822 (1995).
28. Hyer ML*, et al.* A small-molecule inhibitor of the ubiquitin activating enzyme for cancer treatment. *Nature medicine* **24**, 186-193 (2018).
29. Lim KYB, Godde NJ, Humbert PO, Kvansakul M. Structural basis for the differential interaction of Scribble PDZ domains with the guanine nucleotide exchange factor beta-PIX. *J Biol Chem* **292**, 20425-20436 (2017).
30. Doyle DA, Lee A, Lewis J, Kim E, Sheng M, MacKinnon R. Crystal structures of a complexed and peptide-free membrane protein-binding domain: molecular basis of peptide recognition by PDZ. *Cell* **85**, 1067-1076 (1996).
31. Caria S, Stewart BZ, Jin R, Smith BJ, Humbert PO, Kvansakul M. Structural analysis of phosphorylation-associated interactions of human MCC with Scribble PDZ domains. *FEBS J* **286**, 4910-4925 (2019).
32. How JY, Caria S, Humbert PO, Kvansakul M. Crystal structure of the human Scribble PDZ1 domain bound to the PDZ-binding motif of APC. *FEBS Lett* **593**, 533-542 (2019).
33. Javorsky A, Maddumage JC, Mackie ERR, Soares da Costa TP, Humbert PO, Kvansakul M. Structural insight into the Scribble PDZ domains interaction with the oncogenic Human T-cell lymphotrophic virus-1 (HTLV-1) Tax1 PBM. *FEBS J*, (2022).
34. How JY, Stephens RK, Lim KYB, Humbert PO, Kvansakul M. Structural basis of the human Scribble-Vangl2 association in health and disease. *The Biochemical journal* **478**, 1321-1332 (2021).
35. Santoni MJ, Pontarotti P, Birnbaum D, Borg JP. The LAP family: a phylogenetic point of view. *Trends Genet* **18**, 494-497 (2002).
36. Petit MM, Meulemans SM, Alen P, Ayoubi TA, Jansen E, Van de Ven WJ. The tumor suppressor Scrib interacts with the zyxin-related protein LPP, which shuttles between cell adhesion sites and the nucleus. *BMC cell biology* **6**, 1 (2005).
37. Songyang Z*, et al.* Recognition of unique carboxyl-terminal motifs by distinct PDZ domains. *Science* **275**, 73-77 (1997).
38. Janezic EM*, et al.* Scribble co-operatively binds multiple alpha1D-adrenergic receptor C-terminal PDZ ligands. *Sci Rep* **9**, 14073 (2019).
39. Ren J, Feng L, Bai Y, Pei H, Yuan Z, Feng W. Interdomain interface-mediated target recognition by the Scribble PDZ34 supramodule. *The Biochemical journal* **468**, 133-144 (2015).
40. Choy E*, et al.* Endomembrane trafficking of ras: the CAAX motif targets proteins to the ER and Golgi. *Cell* **98**, 69-80 (1999).
41. Dukes JD, Whitley P, Chalmers AD. The MDCK variety pack: choosing the right strain. *BMC Cell Biol* **12**, 43 (2011).

42. O'Brien LE, Zegers MM, Mostov KE. Opinion: Building epithelial architecture: insights from three-dimensional culture models. *Nat Rev Mol Cell Biol* **3**, 531-537 (2002).
43. Roh MH, Fan S, Liu CJ, Margolis B. The Crumbs3-Pals1 complex participates in the establishment of polarity in mammalian epithelial cells. *J Cell Sci* **116**, 2895-2906 (2003).
44. Hurd TW, Fan S, Liu CJ, Kweon HK, Hakansson K, Margolis B. Phosphorylation-dependent binding of 14-3-3 to the polarity protein Par3 regulates cell polarity in mammalian epithelia. *Curr Biol* **13**, 2082-2090 (2003).
45. Shin K, Straight S, Margolis B. PATJ regulates tight junction formation and polarity in mammalian epithelial cells. *J Cell Biol* **168**, 705-711 (2005).
46. Kim M, Datta A, Brakeman P, Yu W, Mostov KE. Polarity proteins PAR6 and aPKC regulate cell death through GSK-3beta in 3D epithelial morphogenesis. *J Cell Sci* **120**, 2309-2317 (2007).
47. Brady DC, Alan JK, Madigan JP, Fanning AS, Cox AD. The transforming Rho family GTPase Wrch-1 disrupts epithelial cell tight junctions and epithelial morphogenesis. *Mol Cell Biol* **29**, 1035-1049 (2009).
48. Rehder D*, et al.* Junctional adhesion molecule-a participates in the formation of apico-basal polarity through different domains. *Exp Cell Res* **312**, 3389-3403 (2006).
49. Iden S*, et al.* aPKC phosphorylates JAM-A at Ser285 to promote cell contact maturation and tight junction formation. *J Cell Biol* **196**, 623-639 (2012).
50. Zhan L*, et al.* Deregulation of scribble promotes mammary tumorigenesis and reveals a role for cell polarity in carcinoma. *Cell* **135**, 865-878 (2008).
51. Yates LL*, et al.* Scribble is required for normal epithelial cell-cell contacts and lumen morphogenesis in the mammalian lung. *Dev Biol* **373**, 267-280 (2013).
52. Horikoshi Y*, et al.* Interaction between PAR-3 and the aPKC-PAR-6 complex is indispensable for apical domain development of epithelial cells. *J Cell Sci* **122**, 1595-1606 (2009).
53. Cohen D, Fernandez D, Lazaro-Dieguez F, Musch A. The serine/threonine kinase Par1b regulates epithelial lumen polarity via IRSp53-mediated cell-ECM signaling. *J Cell Biol* **192**, 525-540 (2011).
54. Durgan J, Kaji N, Jin D, Hall A. Par6B and atypical PKC regulate mitotic spindle orientation during epithelial morphogenesis. *J Biol Chem* **286**, 12461-12474 (2011).
55. Fabrini R*, et al.* Monomer-dimer equilibrium in glutathione transferases: a critical re-examination. *Biochemistry* **48**, 10473-10482 (2009).
56. Legouis R, Jaulin-Bastard F, Schott S, Navarro C, Borg JP, Labouesse M. Basolateral targeting by leucine-rich repeat domains in epithelial cells. *EMBO Rep* **4**, 1096-1102 (2003).
57. Zeitler J, Hsu CP, Dionne H, Bilder D. Domains controlling cell polarity and proliferation in the Drosophila tumor suppressor Scribble. *J Cell Biol* **167**, 1137-1146 (2004).
58. Navarro C*, et al.* Junctional recruitment of mammalian Scribble relies on E-cadherin engagement. *Oncogene* **24**, 4330-4339 (2005).

59. Elsum IA, Humbert PO. Localization, not important in all tumor-suppressing properties: a lesson learnt from scribble. *Cells Tissues Organs* **198**, 1-11 (2013).
60. Chen B*, et al.* ZDHHC7-mediated S-palmitoylation of Scribble regulates cell polarity. *Nat Chem Biol* **12**, 686-693 (2016).
61. Wan S*, et al.* Cytoplasmic localization of the cell polarity factor scribble supports liver tumor formation and tumor cell invasiveness. *Hepatology* **67**, 1842-1856 (2018).
62. Albertson R, Chabu C, Sheehan A, Doe CQ. Scribble protein domain mapping reveals a multistep localization mechanism and domains necessary for establishing cortical polarity. *J Cell Sci* **117**, 6061-6070 (2004).
63. Kobe B, Deisenhofer J. A structural basis of the interactions between leucine-rich repeats and protein ligands. *Nature* **374**, 183-186 (1995).
64. Troyanovsky RB, Indra I, Kato R, Mitchell BJ, Troyanovsky SM. Basolateral protein Scribble binds phosphatase PP1 to establish a signaling network maintaining apicobasal polarity. *J Biol Chem* **297**, 101289 (2021).
65. Mojica W, Hawthorn L. Normal colon epithelium: a dataset for the analysis of gene expression and alternative splicing events in colon disease. *BMC Genomics* **11**, 5 (2010).
66. Lopez-Dee ZP*, et al.* Thrombospondin-1 in a Murine Model of Colorectal Carcinogenesis. *PLoS ONE* **10**, e0139918 (2015).
67. Roberts DL, O'Dwyer ST, Stern PL, Renehan AG. Global gene expression in pseudomyxoma peritonei, with parallel development of two immortalized cell lines. *Oncotarget* **6**, 10786-10800 (2015).
68. Luo D, Yang J, Liu J, Yong X, Wang Z. Identification of four novel hub genes as monitoring biomarkers for colorectal cancer. *Hereditas* **159**, 11 (2022).
69. Wang B*, et al.* Distinguishing colorectal adenoma from hyperplastic polyp by WNT2 expression. *J Clin Lab Anal* **35**, e23961 (2021).
70. Lee J*, et al.* Profiles of microRNA networks in intestinal epithelial cells in a mouse model of colitis. *Sci Rep* **5**, 18174 (2015).
71. Hou J, Karin M, Sun B. Targeting cancer-promoting inflammation - have anti-inflammatory therapies come of age? *Nat Rev Clin Oncol* **18**, 261-279 (2021).
72. Keegan K, Cooper JA. Use of the two hybrid system to detect the association of the protein-tyrosine-phosphatase, SHPTP2, with another SH2-containing protein, Grb7. *Oncogene* **12**, 1537-1544 (1996).
73. Ebnet K, Schulz CU, Meyer Zu Brickwedde MK, Pendl GG, Vestweber D. Junctional adhesion molecule interacts with the PDZ domain-containing proteins AF-6 and ZO-1. *J Biol Chem* **275**, 27979-27988 (2000).
74. Rautureau GJ, Yabal M, Yang H, Huang DC, Kvansakul M, Hinds MG. The restricted binding repertoire of Bcl-B leaves Bim as the universal BH3-only prosurvival Bcl-2 protein antagonist. *Cell Death Dis* **3**, e443 (2012).

75. Evan GI, Lewis GK, Ramsay G, Bishop JM. Isolation of monoclonal antibodies specific for human c-myc proto-oncogene product. *Molecular and cellular biology* **5**, 3610-3616 (1985).
76. Schiestl RH, Gietz RD. High efficiency transformation of intact yeast cells using single stranded nucleic acids as a carrier. *Curr Genet* **16**, 339-346 (1989).
77. Tuncay H*, et al.* JAM-A regulates cortical dynein localization through Cdc42 to control planar spindle orientation during mitosis. *Nature communications* **6**, 8128 (2015).
78. Scopes RK. Measurement of protein by spectrophotometry at 205 nm. *Anal Biochem* **59**, 277-282 (1974).
79. Zhang Y*, et al.* Convergent and divergent ligand specificity among PDZ domains of the LAP and zonula occludens (ZO) families. *J Biol Chem* **281**, 22299-22311 (2006).
80. Maddumage JC, Stewart BZ, Humbert PO, Kvansakul M. Crystallographic Studies of PDZ Domain-Peptide Interactions of the Scribble Polarity Module. *Methods in molecular biology (Clifton, NJ* **2256**, 125-135 (2021).
81. Beilsten-Edmands J, Winter G, Gildea R, Parkhurst J, Waterman D, Evans G. Scaling diffraction data in the DIALS software package: algorithms and new approaches for multi-crystal scaling. *Acta Crystallogr D Struct Biol* **76**, 385-399 (2020).
82. Winn MD*, et al.* Overview of the CCP4 suite and current developments. *Acta Crystallogr D Biol Crystallogr* **67**, 235-242 (2011).
83. Winter G, Lobley CM, Prince SM. Decision making in xia2. *Acta Crystallogr D Biol Crystallogr* **69**, 1260-1273 (2013).
84. McCoy AJ. Solving structures of protein complexes by molecular replacement with Phaser. *Acta Crystallogr D Biol Crystallogr* **63**, 32-41 (2007).
85. Afonine PV*, et al.* Towards automated crystallographic structure refinement with phenix.refine. *Acta Crystallogr D Biol Crystallogr* **68**, 352-367 (2012).
86. Emsley P, Lohkamp B, Scott WG, Cowtan K. Features and development of Coot. *Acta Crystallogr D Biol Crystallogr* **66**, 486-501 (2010).
87. Morin A*, et al.* Collaboration gets the most out of software. *Elife* **2**, e01456 (2013).
88. Meyer PA*, et al.* Data publication with the structural biology data grid supports live analysis. *Nature communications* **7**, 10882 (2016).
89. Pollard DA, Pollard TD, Pollard KS. Empowering statistical methods for cellular and molecular biologists. *Mol Biol Cell* **30**, 1359-1368 (2019).

Figures

Figure 1

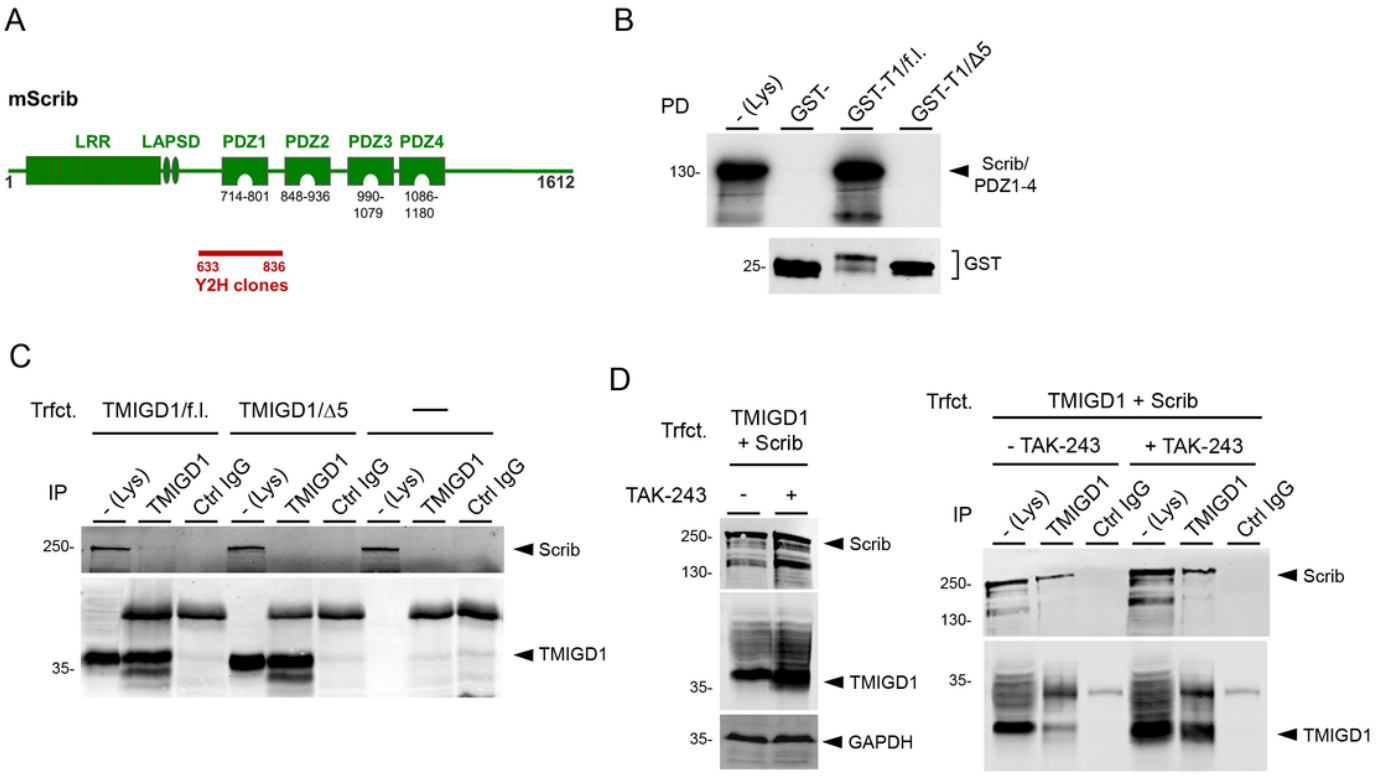

Figure 1

Scrib interacts with TMIGD1. (**A**) Schematic organization of murine Scrib. The region isolated in several independent cDNA clones from a Y2H library that interacted with TMIGD1 (AA 645-814) is depicted by a red bar. Nomenclature refers to isoform 1 of murine Scrib. Abbreviations: LAP, leucine-rich repeat and PDZ domains, LAPSD, LAP-specific domain; LRR, leucine-rich repeat; Y2H, yeast-two hybrid. (**B**) GST pulldown. Top panel: GST-TMIGD1 fusion proteins containing the entire cytoplasmic domain of TMIGD1 (GST-T1) or a deletion mutant lacking the PBM (GST-T1/Δ5) were immobilized and incubated with a Scrib/PDZ1-4 construct generated in vitro by a coupled transcription/translation system in the presence of ^{35}S-methionine. Bound proteins were analyzed by autoradiography. Bottom panel: Loading control of GST fusion proteins used in the pulldown experiments. Proteins were visualized with anti-GST antibodies by Western blotting. Abbreviations: PD, pulldown; leucine-rich repeat and PDZ domains, (**C**) CoIP from HEK293 cells stably transfected with TMIGD1 constructs (TMIGD1/f.l., TMIGD1/Δ5) or untransfected HEK293 cells. (**D**) CoIP from HEK293 cells transfected with TMIGD1 and Scrib in the presence of TAK-243. Left panel: Western blot analysis of cell lysates. Right panel: CoIP. IPs were performed with anti-TMIGD1 antibodies, immunoprecipitates were blotted with antibodies against Scrib or against TMIGD1 (10% input), as indicated. Abbreviations: Ctrl, control; Lys, lysate; IP, immunoprecipitation; TMIGD1/f.l., TMIGD1/full length; TMIGD1/Δ5, TMIGD1 lacking the five C-terminal AA, Trfct., Transfection. Data shown in this figure are representative of 3 independent experiments.

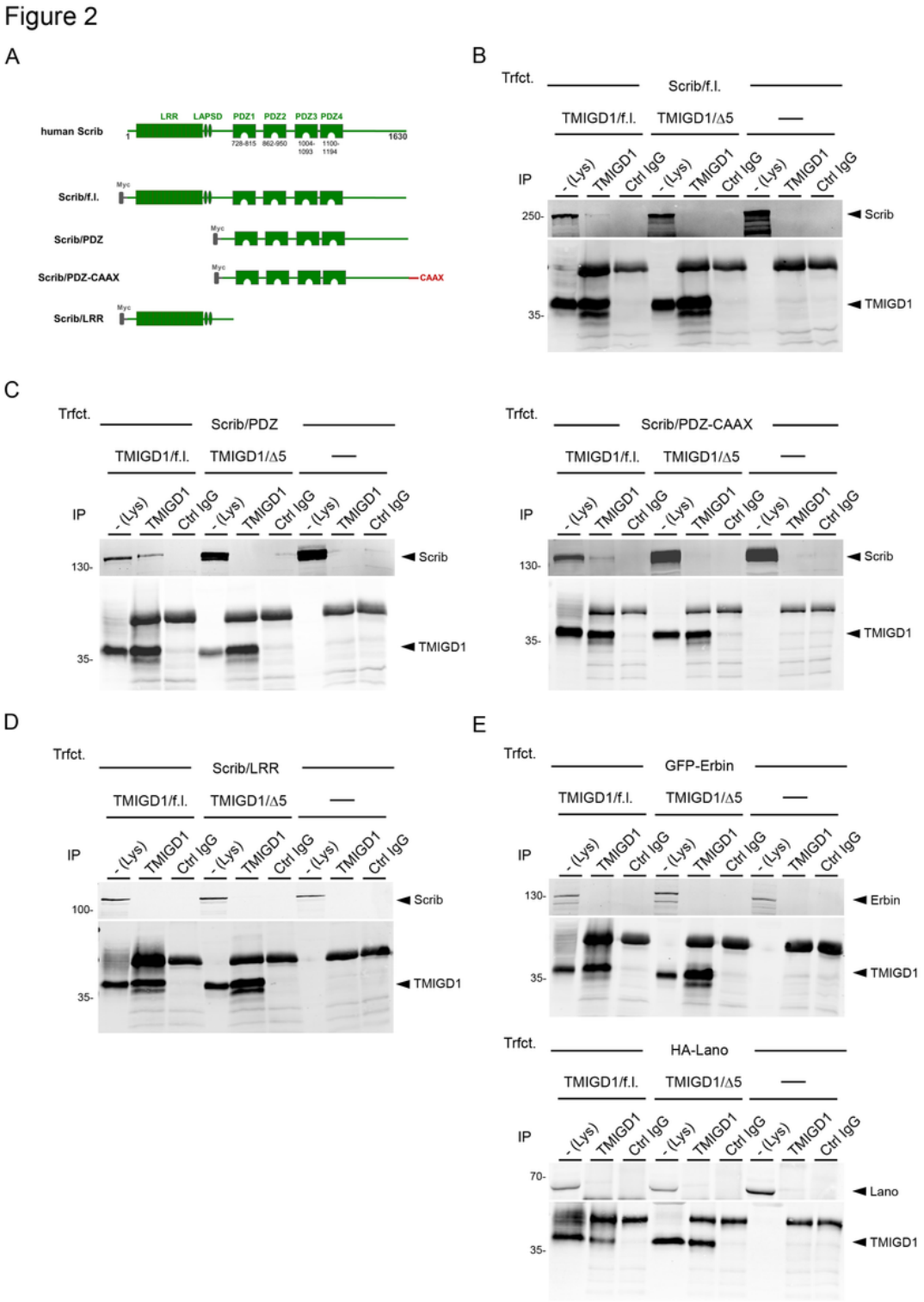

Figure 2

Scrib interacts with TMIGD1 through its PDZ domain region. (**A**) Schematic organization of human Scrib constructs used for mapping experiments. (**B - D**) CoIP experiments with HEK293 cells stably transfected with TMIGD1 constructs (TMIGD1/f.l., TMIGD1/Δ5) or untransfected HEK293 cells and transiently transfected with Scrib constructs shown in the Fig. 2A. In all cases, IPs were performed with anti-TMIGD1 antibodies, immunoprecipitates were blotted with antibodies against Scrib (top panels) or against

TMIGD1 (10% input) as indicated. (**E**) CoIP experiments with HEK293 cells stably transfected with TMIGD1 constructs (TMIGD1/f.l., TMIGD1/Δ5) or untransfected HEK293 cells and transiently transfected with Erbin (top) or Lano/LRRC1 (bottom). IPs were performed with anti-TMIGD1 antibodies, immunoprecipitates were blotted with antibodies against GFP-Erbin (anti-GFP) and TMIGD1 (top) or against HA-Lano/LRRC1 (anti-HA) and TMIGD1 (bottom). Abbreviations: Lys, lysate; IP, immunoprecipitation; Trfct., transfection. Data shown in this figure are representative of 3 independent experiments.

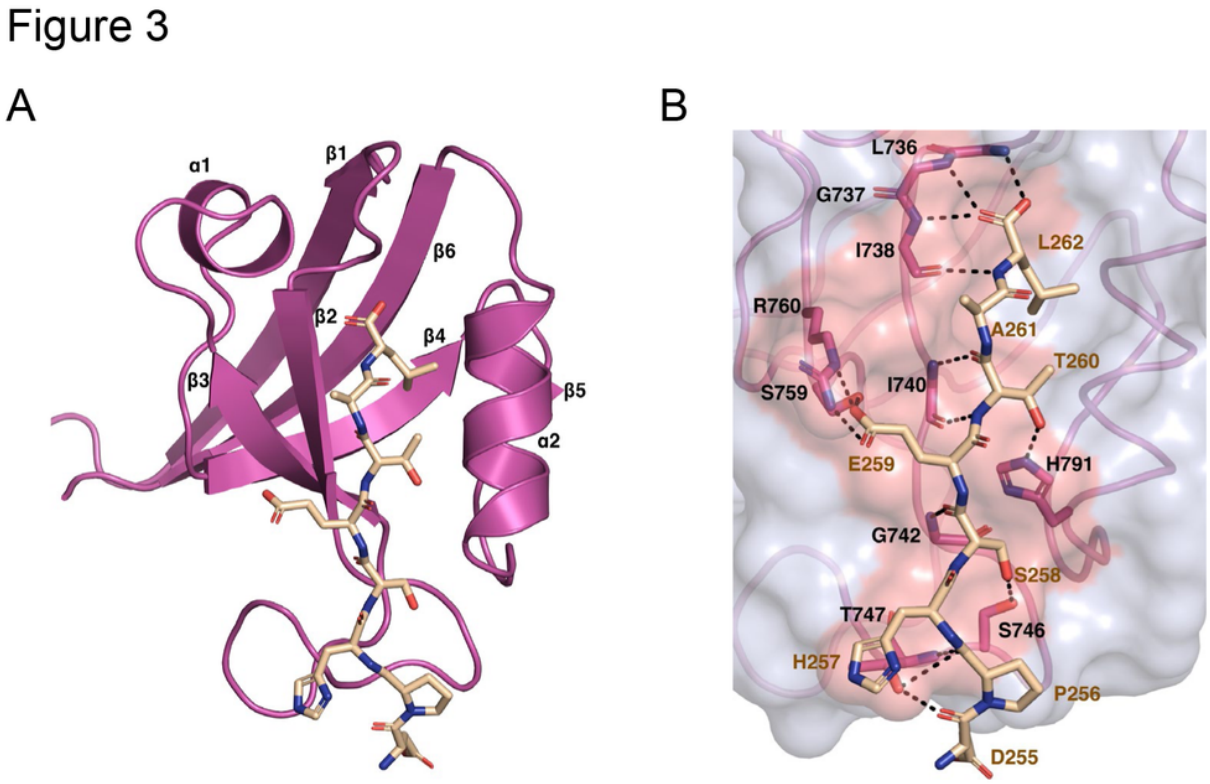

Figure 3

Crystal structure of the human Scrib/PDZ1 – human TMIGD1 PBM complex. (**A**) Human Scrib/PDZ1 (light magenta, represented as simplified ribbon diagram, “cartoon”) in complex with the human TMIGD1 C-terminal peptide (DPHSETAL, cream, represented as sticks). (**B**) Detailed view of the Scrib/PDZ1 – TMIGD1 interface. The PDZ1 surface and the ligand binding groove are shown in light grey and salmon, respectively; the PDZ1 carbon backbone is depicted as sticks in light magenta. The TMIGD1 peptide is depicted as sticks in cream, oxygen atoms are red, nitrogen atoms are blue. Direct contacts between TMIGD1 peptide and Scrib/PDZ1 protein residues are displayed as dashed black lines. AA residues are displayed in single letter code.

Figure 4

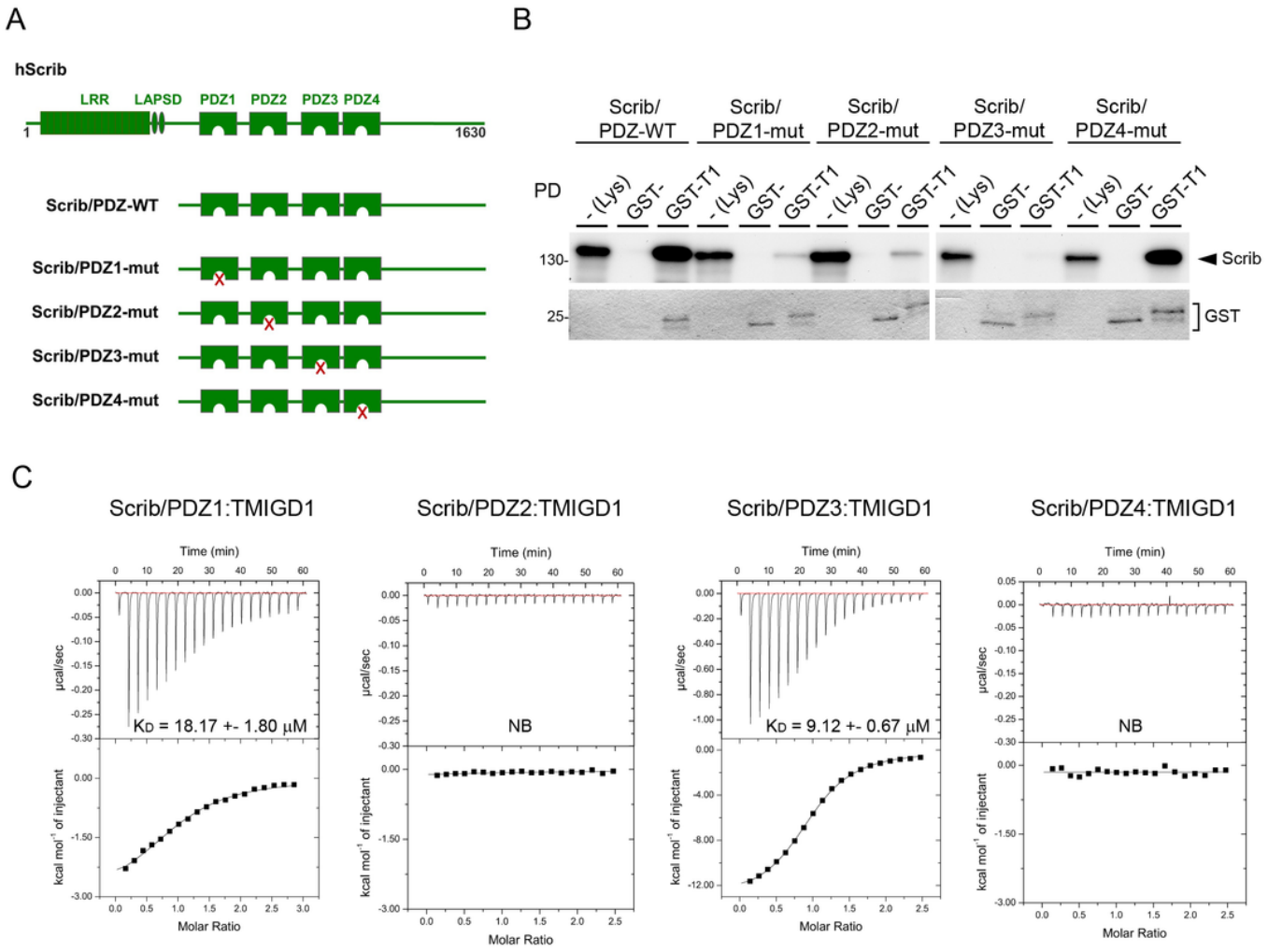

Figure 4

TMIGD1 interacts with Scrib through several PDZ domains. (**A**) Schematic organization of human Scrib PDZ domain constructs with inactivated PDZ domains. Mutated PDZ domains are indicated by red crosses. (**B**) GST pulldown. GST-TMIGD1 fusion proteins were immobilized and incubated with recombinant Scrib proteins with inactivated PDZ domains generated in vitro by a coupled transcription/translation system in the presence of ^{35}S-methionine. Bound proteins were analyzed by autoradiography. Bottom panel: Loading control of GST fusion proteins used in the pulldown experiments. Proteins were visualized by staining with Coomassie Brilliant Blue. Abbreviations: GST-T1, GST-TMIGD1; PD, pulldown. Data are representative of 3 independent experiments. (**C**) Interaction profiles of hScrib PDZ domains with hTMIGD1 peptide. Each profile is depicted by a raw thermogram (top part) and binding isotherm fitted with a one-site binding mode (bottom). Abbreviations: K_D, dissociation constant ± standard deviation (SD); NB, no binding. Each value was calculated from at least three independent experiments.

Figure 5

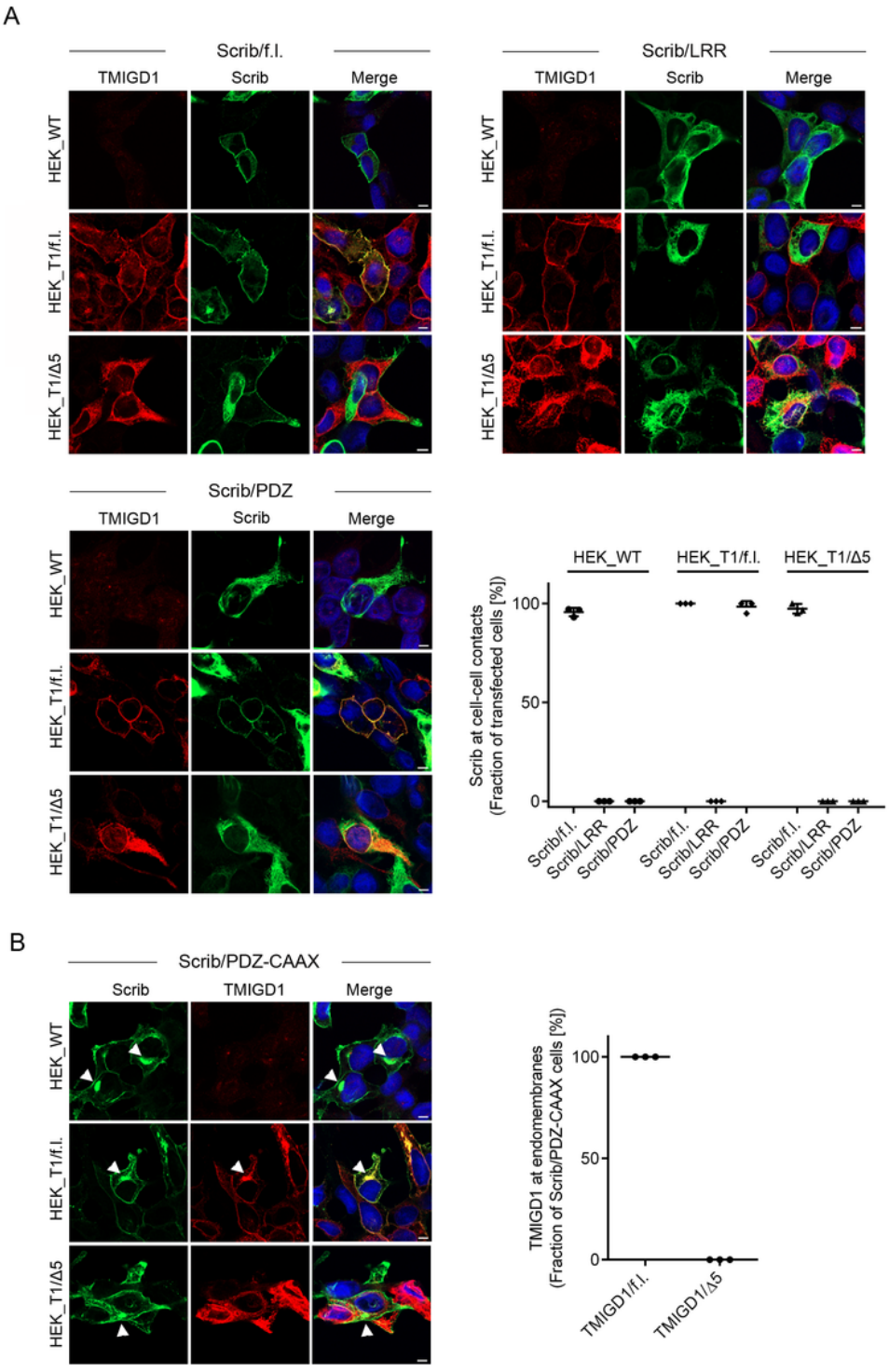

Figure 5

TMIGD1 recruits Scrib to cell-cell contacts. (**A**) HEK293 cells, either untransfected (HEK293 WT) or stably transfected with TMIGD1/full length (HEK_T1/f.l.) or with TMIGD1 lacking the PDZ domain motif (HEK_T1/Δ5) were transiently transfected with the indicated Scrib mutant constructs and stained for TMIGD1 and Scrib. Note that Scrib/f.l. localizes to cell-cell contacts in the absence of TMIGD1 (HEK_WT), but that Scrib/PDZ localization at cell-cell contacts depends on TMIGD1 and is mediated by the PDZ

domain motif of TMIGD1. Quantification of Scrib recruitment to cell-cell contacts. The dot plot graph shows the fraction of cells with Scrib localization at cell-cell contacts. Scrib/f.l.: n = 81 (TMIGD1/f.l.), n = 76 (TMIGD1/Δ5); Scrib/LRR: n = 64 (TMIGD1/f.l.), n = 63 (TMIGD1/Δ5); Scrib/PDZ: n = 68 (TMIGD1/f.l.), n = 72 (TMIGD1/Δ5); N = 3 independent experiments, represented by individual dots. Scale bars: 5 µm. (**B**) HEK293 cell lines described in (A) were transiently transfected with a Scrib/PDZ-CAAX construct and stained for TMIGD1 and Scrib. Note that the Scrib/PDZ-CAAX localizes to endomembrane structures (arrowheads), and that TMIGD1/f.l., but not TMIGD1/Δ5 co-localizes with Scrib/PDZ-CAAX at endomembranes. Right: Quantification of TMIGD1 co-localization with Scrib/PDZ-CAAX at endomembranes. The graph shows the fraction of Scrib/PDZ-CAAX-transfected cells with TMIGD1 localization at endomembranes. TMIGD1/f.l.: n = 81, TMIGD1/Δ5: n = 76. N = 3 independent experiments, represented by individual dots. Scale bars: 5 µm.

Figure 6

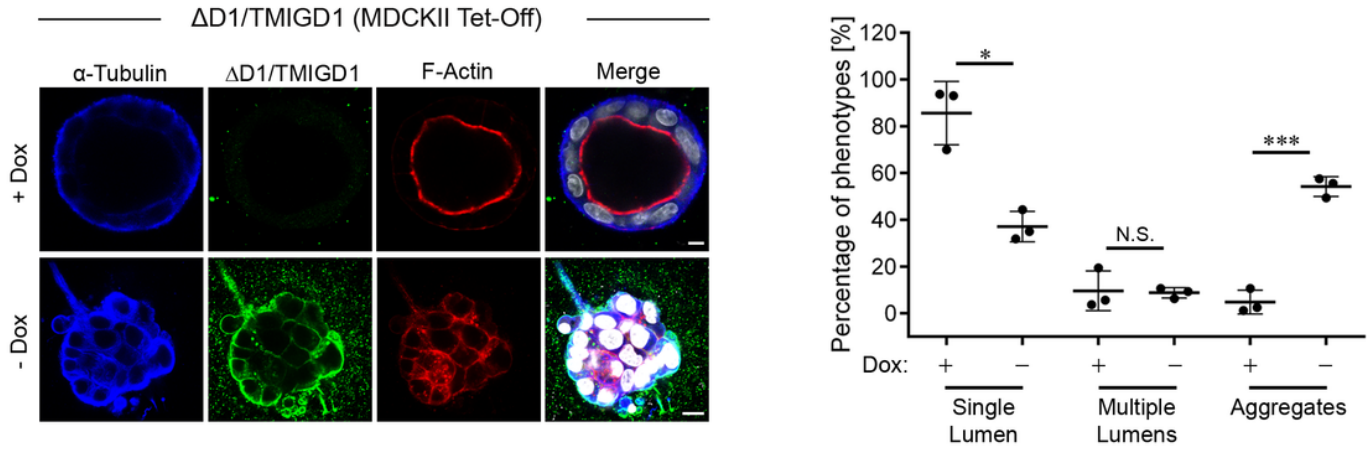

Figure 6

ΔD1-TMIGD1 impairs lumen formation in MDCKII cysts. MDCKII cells stably transfected with a TMIGD1 construct lacking the membrane-distal Ig-like domain (ΔD1/TMIGD1) under a doxycycline (Dox)-regulated promoter were left uninduced (+ Dox) or were induced by Dox removal (- Dox), and cultured for 6 days in a three-dimensional collagen matrix. Cysts were stained for α-tubulin, ΔD1/TMIGD1 (anti Flag tag) and F-actin, DNA was stained with DAPI. Scale bars: 5 µm. The dot plot shows the quantification of lumen formation. Cyst phenotypes were categorized into cysts with single lumen (Single Lumen), cysts with multiple lumens (Multiple Lumens), and multicellular aggregates without lumen (Aggregates). Statistical evaluation was performed with unpaired Student's t-test. Data are represented as means ± SD (n = 980, N = 3 independent experiments). N.S., not significant, *p < 0.05, ***p < 0.001.

Supplementary Files

This is a list of supplementary files associated with this preprint. Click to download.

- SupplementaryMaterial.pdf